Mechanochemical Removal of Ribosome Biogenesis Factors from Nascent 60S Ribosomal Subunits

Cell

Mechanochemical Removal of Ribosome Biogenesis Factors from Nascent 60S Ribosomal Subunits

Cornelia Ulbrich,[1,4] Meikel Diepholz,[2,4] Jochen Baßler,[1,4] Dieter Kressler,[1] Brigitte Pertschy,[1] Kyriaki Galani,[1,2] Bettina Böttcher,[2,3,*] and Ed Hurt[1,*]

[1]Biochemie-Zentrum der Universität Heidelberg, Im Neuenheimer Feld 328, 69120 Heidelberg, Germany
[2]EMBL, Meyerhofstrasse 1, 69117 Heidelberg, Germany
[3]University of Edinburgh, School of Biological Sciences, King's Buildings, Mayfield Road, Edinburgh EH9 3JR, UK
[4]These authors contributed equally to this work
*Correspondence: ed.hurt@bzh.uni-heidelberg.de (E.H.), bettina.boettcher@ed.ac.uk (B.B.)
DOI 10.1016/j.cell.2009.06.045

SUMMARY

The dynein-related AAA ATPase Rea1 is a preribosomal factor that triggers an unknown maturation step in 60S subunit biogenesis. Using electron microscopy, we show that Rea1's motor domain is docked to the pre-60S particle and its tail-like structure, harboring a metal ion-dependent adhesion site (MIDAS), protrudes from the preribosome. Typically, integrins utilize a MIDAS to bind extracellular ligands, an interaction that is strengthened under applied tensile force. Likewise, the Rea1 MIDAS binds the preribosomal factor Rsa4, which is located on the pre-60S subunit at a site that is contacted by the flexible Rea1 tail. The MIDAS-Rsa4 interaction is essential for ATP-dependent dissociation of a group of nonribosomal factors from the pre-60S particle. Thus, Rea1 aligns with its interacting partners on the preribosome to effect a necessary step on the path to the export-competent 60S subunit.

INTRODUCTION

The assembly of eukaryotic ribosomal subunits, which are composed of ribosomal RNA (25S/28S, 18S, 5.8S, and 5S rRNA) and about 80 ribosomal proteins, takes successively place in the nucleolus, nucleoplasm and cytoplasm. This complicated process is initiated by transcription of a large pre-rRNA precursor, which is subsequently modified, processed and assembled with the ribosomal proteins. At the beginning of ribosome synthesis, a huge (90S) precursor particle is formed that is then split to induce the formation of the pre-60S and pre-40S particles, which each follow separate biogenesis and export routes (Fromont-Racine et al., 2003; Granneman and Baserga, 2004; Henras et al., 2008; Tschochner and Hurt, 2003; Zemp and Kutay, 2007).

Proteomic approaches have revealed more than 150 non-ribosomal factors, which transiently associate with these nascent 60S and 40S subunits during ribosome biogenesis. It is assumed that these factors drive the multiple maturation steps in a temporally and spatially ordered fashion. Some of these preribosomal factors have domains homologous to ATPases or GTPases suggesting that they trigger energy-consuming steps. Among these types of factors are three AAA-type ATPases that are specifically involved in 60S subunit biogenesis. In general AAA-type ATPases apply force on their substrates upon ATP hydrolysis, which can trigger structural rearrangements or substrate release (Erzberger and Berger, 2006; Vale, 2000). The activity of the AAA ATPase Drg1 is required for the release of shuttling proteins from the pre-60S particles shortly after nuclear export (Pertschy et al., 2007). The other characterized AAA ATPase Rix7 mediates the release of a specific pre-60S factor, Nsa1, from the evolving nascent 60S subunit in the nucleus (Kressler et al., 2008). Finally, the large ~550 kDa AAA ATPase Rea1 (also called Midasin or Mdn1) is associated with pre-60S subunits and its ATPase domain is distantly related to the motor protein dynein heavy chain (Nissan et al., 2002). Rea1 has several distinct domains, an N-terminal extension (35 kDa), followed by an ATPase domain containing six tandem AAA protomers (between 28 and 40 kDa each), a linker domain (260 kDa), a D/E-rich domain (approximately 70 kDa) and a carboxy-terminal domain (30 kDa) that possesses a MIDAS (*m*etal *i*on-*d*ependent *a*dhesion *s*ite), which is homologous to the I-domain of integrins (Garbarino and Gibbons, 2002).

Rea1, which is the largest yeast protein and highly conserved in evolution, was identified as a specific component of an intermediate pre-60S particle that is located in the nucleoplasm and carries the salt-stable Rix1-Ipi3-Ipi1 subcomplex (Galani et al., 2004; Krogan et al., 2004; Nissan et al., 2004). Genetic analyses demonstrated that Rea1, like the members of the Rix1-subcomplex, is required for 60S subunit formation and ITS2 processing, a late pre-rRNA processing step generating the mature 5.8S rRNA from the 7S pre-rRNA (Galani et al., 2004).

Electron microscopic (EM) analysis revealed a tadpole-like shape of the pre-60S particle carrying Rea1 and the Rix1-subcomplex (Nissan et al., 2004). The head region of this particle was assigned to the 60S part and the tail extension was suggested to carry preribosomal factors including Rea1 (Nissan

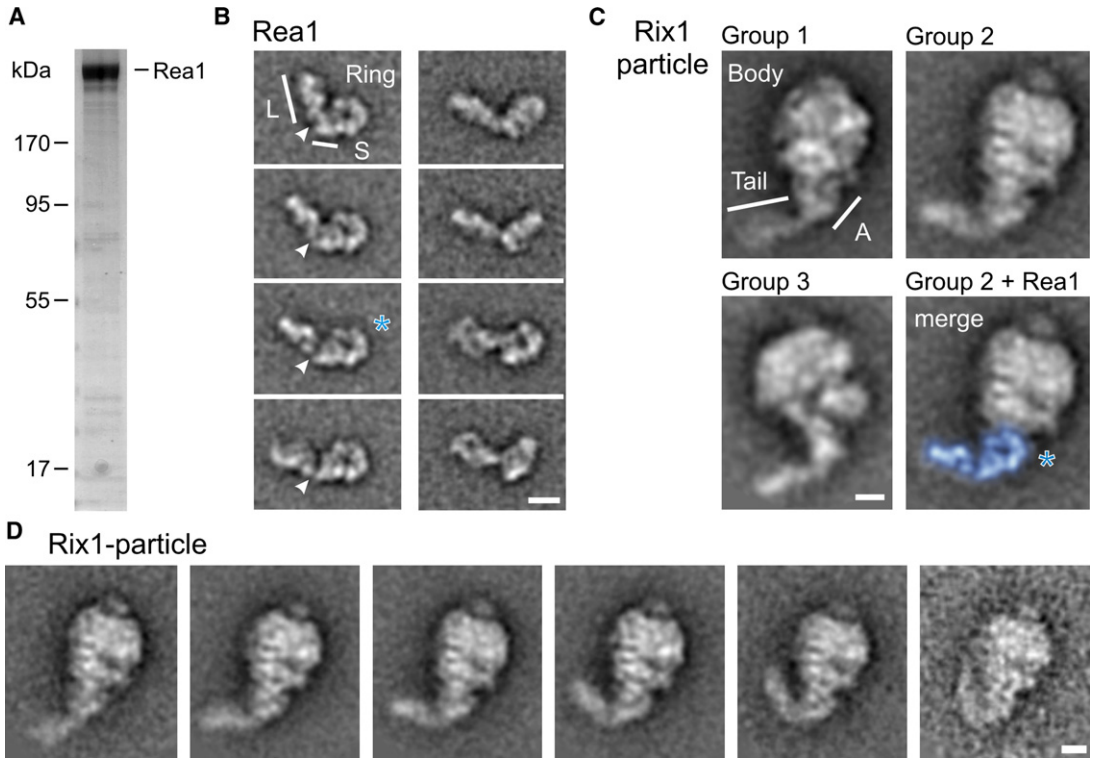

Figure 1. Identification of Position and Dynamics of Rea1 on the Rix1 Pre-60S Particle

(A) Affinity-purified TAP-Rea1 devoid of preribosomal and ribosomal proteins was analyzed by SDS-PAGE and Coomassie staining. Indicated at the left is the molecular weight protein standard in kDa.

(B) Eight representative class averages of the Rea1 molecule. Class averages in the left column show the ring-like shape of the compact domain that connects via a short segment (S) to a longer segment (L) in the elongated tail. The relative orientation of the ring and the short segment does not change significantly, whereas the long tail-segment adopts different positions. The virtual hinge between long segment and short segment is indicated by an arrow-head. The right column shows other orientations of the Rea1 molecule, in which the ring-shaped domain is rotated out of plane. The scale bar represents 10 nm.

(C) The three most representative groups of tail-containing Rix1-particle classes. Major structural landmarks in the Rix1-particle are indicated in group 1 (body, tail and attachment site abbreviated as "A"). Particles that classified into groups 1-3 represent 87% of all tail-containing particles (group 1: 52%, group 2: 24%, and group 3: 11%). For comparison, one Rea1 class average (marked by a blue star in [B]) was overlaid to the tail regions of a group 2 Rix1-particle class average ([C] merge with Rea1*). The overlay shows a good agreement in size and shape between the isolated Rea1 molecule (blue) and the tail and attachment site within the Rix1-particle. The scale bar represents 10 nm.

(D) Movement of the Rea1 tail in the Rix1-particle. Averages of Rix1-particles with the same projection of the body displayed different angular orientations of the tail. The averages are also shown as frames in Movie S2. The first five averages represent one of the five groups in the histogram shown in Figure S2B. The sixth average is a subpopulation of the fifth group in which the tip of the tail appears to make contact to the body of the Rix1-particle. The scale bar represents 10 nm.

et al., 2004). Thus, it was proposed that the AAA ATPase Rea1 could power an ATP-dependent maturation step during 60S subunit formation, but how Rea1 could fulfill this function remained elusive.

Here, we show by electron microscopy that Rea1 consists of two main structural parts, an AAA motor domain, which is stably bound to the pre-60S particle, and a long tail that points away from the preribosome. The Rea1 tail is hinged to the rest of the pre-60S particle enabling the MIDAS at the carboxy-terminal end of the tail to create contact with a distant site on the Rix1 pre-60S particle, where the preribosomal factor Rsa4 is located. Importantly, the Rea1 MIDAS can physically interact with Rsa4. In vivo, site-specific mutants mapping in either the MIDAS or Rsa4 abrogate this interaction and cause a robust 60S subunit export defect. Thus, Rea1 can make contact to the pre-60S subunit at two separate sites, to Rsa4 via the tip of the tail carrying the MIDAS and via the AAA ATPase domain close to the Rix1-complex. In this constellation, the Rea1 motor domain generates force upon ATP hydrolysis to irreversibly remove pre-60S factors, thereby conferring export competence to the pre-60S subunit.

RESULTS

EM Analysis of Isolated Rea1 and of Rea1 Attached to the Rix1-Purified Pre-60S Particle

The conserved AAA ATPase Rea1 is associated with an intermediate pre-60S particle (termed Rix1-particle) in the nucleoplasm that typically carries the salt-stable Rix1-Ipi1-Ipi3 complex (termed Rix1-subcomplex). To elucidate the role of Rea1 in 60S subunit biogenesis, we sought to assign its position within the Rix1-particle. Therefore, we purified Rea1 by tandem affinity-purification (Figure 1A). The negatively stained Rea1 molecules

were examined by EM and single particle analysis (Figure 1B and Table S1 available with this article online). The selected class averages of Rea1 showed an elongated molecule consisting of a ring-like structure with a diameter of 12 ± 1 nm and an elongated "tail" (Figure 1B). The tail consists of a longer (14 ± 1 nm) and a shorter segment (3 ± 1 nm). The latter connects the tail to one side of the ring. Both segments appear to be flexibly hinged as seen in different class averages that show a similar arrangement of the ring and short tail-segment, but different orientations of the long tail-segment (Figure 1B, left column, and Movie S1).

Next, we negatively stained the pre-60S particles purified via the Rix1-TAP bait and calculated class averages. Class averages of the majority of particles (~70%) showed a tadpole-like shape (Nissan et al., 2004) consisting of a tail which is connected via an attachment site to the main body (Figure 1C). More than 85% of the tail-containing particles clustered into only three groups with different views of the body and the tail mostly protruding to one side with a certain degree of flexibility (Figures 1C, 1D, and S1). Class averages of the remaining ~30% of particles did not show a tail and were generally less well defined suggesting greater variability (Figure S1).

Comparison of class averages of the tail-containing pre-60S particles and isolated Rea1 protein showed that the shape of the tail resembled the characteristic shape of purified Rea1 (compare Figures1B and 1C). This observation was further confirmed by overlays between class averages of Rea1 and the Rix1-particle. In these overlays the globular domain of the Rea1 molecule is seen at the attachment site between tail and the body of the pre-60S subunit (Figure 1C, merge with Rea1). This positioning of Rea1 within the Rix1-particle was consistent with earlier antibody labeling that localizes the N-terminus of Rea1, which directly precedes the AAA domain, close to the attachment site in the pre-60S particle (Nissan et al., 2004). Vice versa, the C-terminal MIDAS domain of Rea1 was assumed to be located most distant to the N-terminus at the tip of the Rea1 tail (see Introduction). To test this hypothesis, Rea1 was modified C-terminally with a triple HA-tag, and the affinity-purified Rix1-particle was analyzed by immuno-EM using antibodies against HA. Class averages of labeled Rix1-particles showed enlarged tips of the tails (Figure 2A), thus verifying the localization of the C-terminal MIDAS-domain close to the end of the tail. We conclude that Rea1's globular domain contains the N-terminal domain and the following six AAA-ATPase protomers, whereas the tail consists of the other described motifs (i.e., linker, D/E-rich and MIDAS domains; see Introduction) with MIDAS at or close to the tip of the tail.

It is still unknown where the 60S-moiety is positioned within the body of the Rix1-particle. Therefore, we determined where 60S marker proteins (Rpl) are located within the Rix1-particle. We performed immuno-EM to localize the ribosomal proteins Rpl5, which is part of the central protuberance in the mature 60S subunit, and Rpl3, which is positioned at the opposite side of the 60S moiety (Spahn et al., 2001). For antibody labeling, Rpl3 and Rpl5 were fused to a C-terminal triple HA-tag and functionally expressed in the Rix1-TAP strain. In the class averages of Rix1-particles carrying Rpl3-HA the HA-antibody bound close to the top of the body and pointed to the side of the tail, whereas in the Rpl5-HA carrying pre-60S subunits the extra density of the HA-antibody was detected at the opposite side above the attachment site (Figure 2A). Due to the flexibility of the bound antibody, these class averages showed less detail than class averages of Rix1-particles without bound antibody (Figure 2B). Therefore, we confirmed the significance of this antibody labeling by counting the occurrence of additional densities in a given segment at the periphery of the Rix1-particle in raw images. In all experiments, the segment, in which the extra density was seen in the class averages, contained significantly more peripheral densities than the other five segments (Figure S2A). Taken together this analysis located two spatially distant Rpl proteins of the 60S moiety and placed the central protuberance close to the AAA ATPase domain of Rea1.

Since it was hypothesized that Rea1 could bind via the Rix1-subcomplex to the 60S subunit (Nissan et al., 2004), we aimed to determine the position of Rix1, Ipi1 and Ipi3 by antibody labeling of HA-tagged proteins in negatively stained pre-60S particles. Whereas the antibody against Rix1-HA was found close to the globular domain of Rea1, the antibody against Ipi3-HA was located above Rix1 and close to Rpl5 (Figures 2A and 2C). Ipi1 could not be localized due to inefficient labeling (data not shown). These data suggest that the Rix1-subcomplex is sandwiched between the AAA-ATPase domain and the 60S subunit joining surface and thus could serve as possible adaptor between these two entities.

A Flexible Rea1 Tail Could Bring the MIDAS in Proximity to Rsa4 to Allow a MIDAS-Rsa4 Contact

Class averages with similar projections of the body of the Rix1-particle often displayed the tail in different angles with respect to the main axis of the body, suggesting flexibility of the tail. To quantify this flexibility further, we grouped particles with the same projection of the body by supervised classification and sub-classified these particles according to the features in the tail region by multivariate statistical analysis. The largest flexibility was observed for 'Group 2' Rix1-particles (see Figure 1C). Their class averages indicated that Rea1's tail is flexible around a virtual hinge close to the AAA ATPase domain (Figure 1D and Movie S2) and covers an angular range of ~120° (Figure S2B). The favored orientation of the tail is in the middle of this angular range. In a few particles the tip of the tail comes close to the pre-60S body and may even contact a discrete region on the pre-60S subunit, which is below the location of Rpl3, but distant to the binding site of the Rea1 AAA ATPase domain (Figure 1D). Since the tail region of Rea1 contains the MIDAS, a well-known motif mediating protein-protein interaction, it is possible that the tail movement brings the MIDAS close to another factor on the pre-60S particle to allow for a direct contact.

To find out if the Rea1 MIDAS indeed could develop a physical connection to a second site on the pre-60S subunit, we searched for factors that interact with the Rea1 MIDAS domain. Valid candidates are proteins, which co-purify with the Rix1-particle. In the past, several factors have been reported to be associated with the Rix1-particle. Re-investigation of these bands by SDS-PAGE of the purified Rix1-particle confirmed that the Rix1-Ipi1-Ipi3 subcomplex is highly enriched (Figure 3A). Additional prominent bands in the Rix1-particle were Rea1, Rsa4, Nsa2, Arx1 and the GTPases Nog1, Nog2 and Nug1 (Galani et al., 2004;

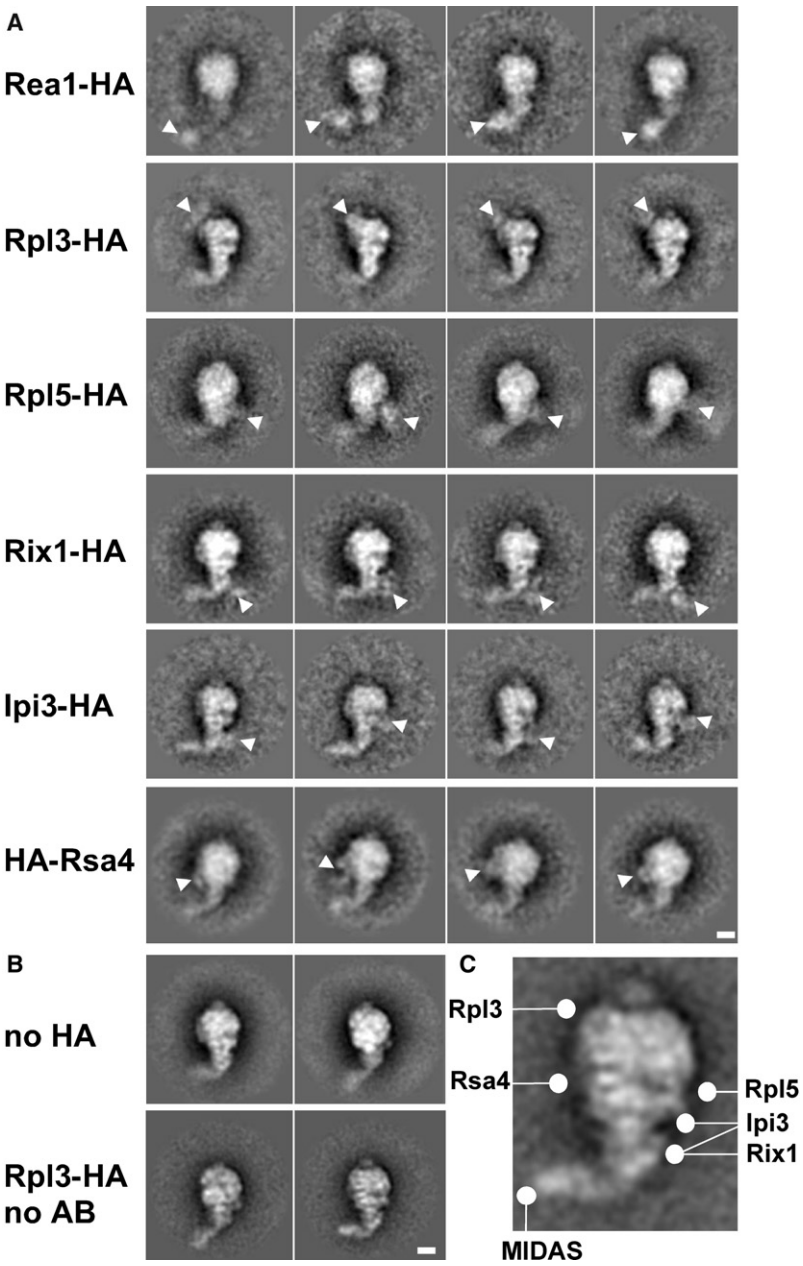

Figure 2. Positioning of Ribosomal Proteins and Preribosomal Factors on the Rix1-Particle

(A) Class averages of HA-antibody labeled negatively stained Rix1-particles purified via the Rix1-TAP bait. The HA-labeled protein is indicated on the left. Rea1, Rpl5 and Rpl3 carried a C-terminal HA-tag, Rsa4 had an N-terminal HA-tag. In the case of Rix1 and Ipi3, the HA-tag was inserted at the C terminus before the TAP-tag. Ipi3-TAP was shown to purify the same particles as Rix1-TAP (Nissan et al., 2004). White arrowheads indicate the position of the antibody-dependent extra density.

(B) Negative controls for antibody labeling. Class averages of Rix1-particles that did not carry the HA-tag but were incubated with HA-antibodies (upper row). No extra density of a contaminating antibody is visible. Rix1-particles containing the HA-tag on Rpl3 were affinity-purified without the HA-antibody (lower row). The scale bar represents 10 nm.

(C) Class average of the Rix1-particle with the approximate positions of all localized proteins.

Nissan et al., 2002; Nissan et al., 2004). Western blotting revealed that Rsa4 and Nog2 co-purified mainly with the Rix1-particle, whereas Nog1, Nsa2 and Tif6 were also found in earlier and later pre-60S particles (Figure 3B).

To identify the factor(s) present on the Rix1-particle that potentially could bind to the MIDAS in the Rea1 tail, we performed yeast 2-hybrid assays. Among the analyzed factors, only Rsa4 exhibited a robust 2-hybrid interaction with the Rea1 MIDAS bait, whereas Nog2, Nog1, Nsa2, Rix1, Ipi3, and Ipi1 did not interact (Figure 3C). Further investigations demonstrated that the domain with the predicted MIDAS fold (residues 4700-4910 in Rea1) plus an adjacent sequence (4620-4699) and the highly conserved N-domain of Rsa4 (residues 20-128) were necessary for the 2-hybrid interaction (Figure 4A, see also Figures S3A, S3B, S4A, and data not shown). Consistent with this finding, NOTCHLESS, the plant homolog of Rsa4, exhibits a 2-hybrid interaction with the Rea1 homolog Midasin (Chantha and Matton, 2006). To test whether Rsa4 and Rea1 can directly interact, we co-expressed His-Rsa4 and GST-MIDAS in *E. coli*. Affinity-purification of GST-MIDAS from a bacterial lysate revealed a strong co-enrichment of Rsa4 (Figure 4B) showing that the MIDAS of Rea1 binds directly to Rsa4.

To determine whether the position of Rsa4 within the Rix1-particle could be consistent with a physical interaction between Rsa4 and the Rea1 MIDAS, we performed immuno-EM as described above. This analysis showed that HA-Rsa4 is located in the center of the body pointing to the side of the tail (Figures 2 and S2A). The area defined by antibody labeling of Rsa4 overlaps with the site where the tail contacts the body of the Rix1-particle (Figure 1D). Altogether, these data indicate that a movement of the Rea1 tail brings the Rea1 MIDAS in proximity to Rsa4 and thus could allow in vivo a physical contact between these two proteins on the pre-60S subunit.

The Rea1 MIDAS-Rsa4 Interaction Resembles the Classical Integrin MIDAS-Ligand Interaction

To investigate the mechanism by which the Rea1 MIDAS binds to Rsa4, we took advantage of the structural knowledge of how an integrin MIDAS interacts with its ligand (i.e., extracellular matrix protein). Crystal structures of MIDAS-ligand complexes show that the MIDAS ion (mainly Mg^{2+}) at the integrin–ligand interface is coordinated by five conserved residues of the MIDAS fold (consensus DxSxS-x_{70}-T-x_{30}-(S/T)DG) and the sixth coordination residue (either E or D) is provided by the ligand (Arnaout

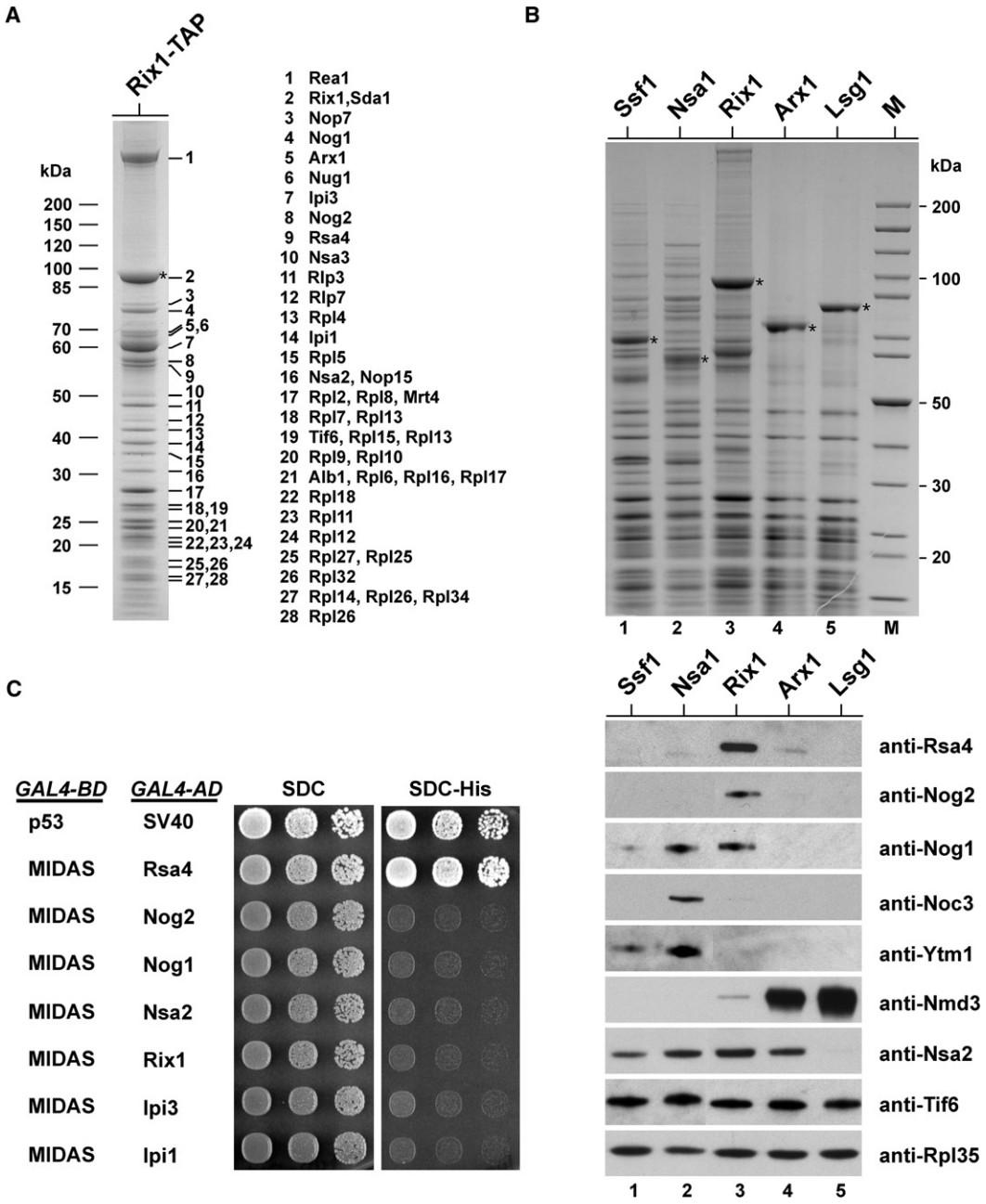

Figure 3. Rsa4 Associates with the Rix1 Pre-60S Particle and Interacts with the Rea1 MIDAS in the 2-Hybrid Assay

(A) Protein composition of the pre-60S particle used for electron microscopic analysis. The final EGTA eluate of Rix1-TAP was analyzed by 4%–12% gradient SDS-PAGE and Coomassie staining. The indicated protein bands (1 to 28) were identified by mass spectrometry.

(B) Rsa4 and Nog2 are co-enriched within the Rix1 pre-60S particle. The final eluates of tandem affinity purifications (TAP) using the bait proteins Ssf1, Nsa1, Rix1, Arx1 and Lsg1 were analyzed by SDS-PAGE and Coomassie staining (upper panel, lanes 1-5) and western blotting using the indicated antibodies (lower panel). M, molecular weight protein standard. The asterisks mark the positions of the bait proteins.

(C) 2-hybrid analysis reveals an interaction of the Rea1 MIDAS (residues 4620-4910) with Rsa4, but not with other pre-60S factors. 2-hybrid plasmids expressing the indicated *GAL4-BD* (*GAL4* DNA binding domain) and *GAL4-AD* (*GAL4* activation domain) constructs were transformed into the yeast reporter strain PJ69-4A. Transformants were spotted in 10-fold serial dilutions onto SDC-Trp-Leu (SDC) or SDC-Trp-Leu-His (SDC-His) plates. Expression of the *HIS3* marker allows growth on SDC-His plates and thus indicates a 2-hybrid interaction. Plates were incubated for 4 days at 30°C. The combination of p53 and the SV40 large T-antigen served as a positive control.

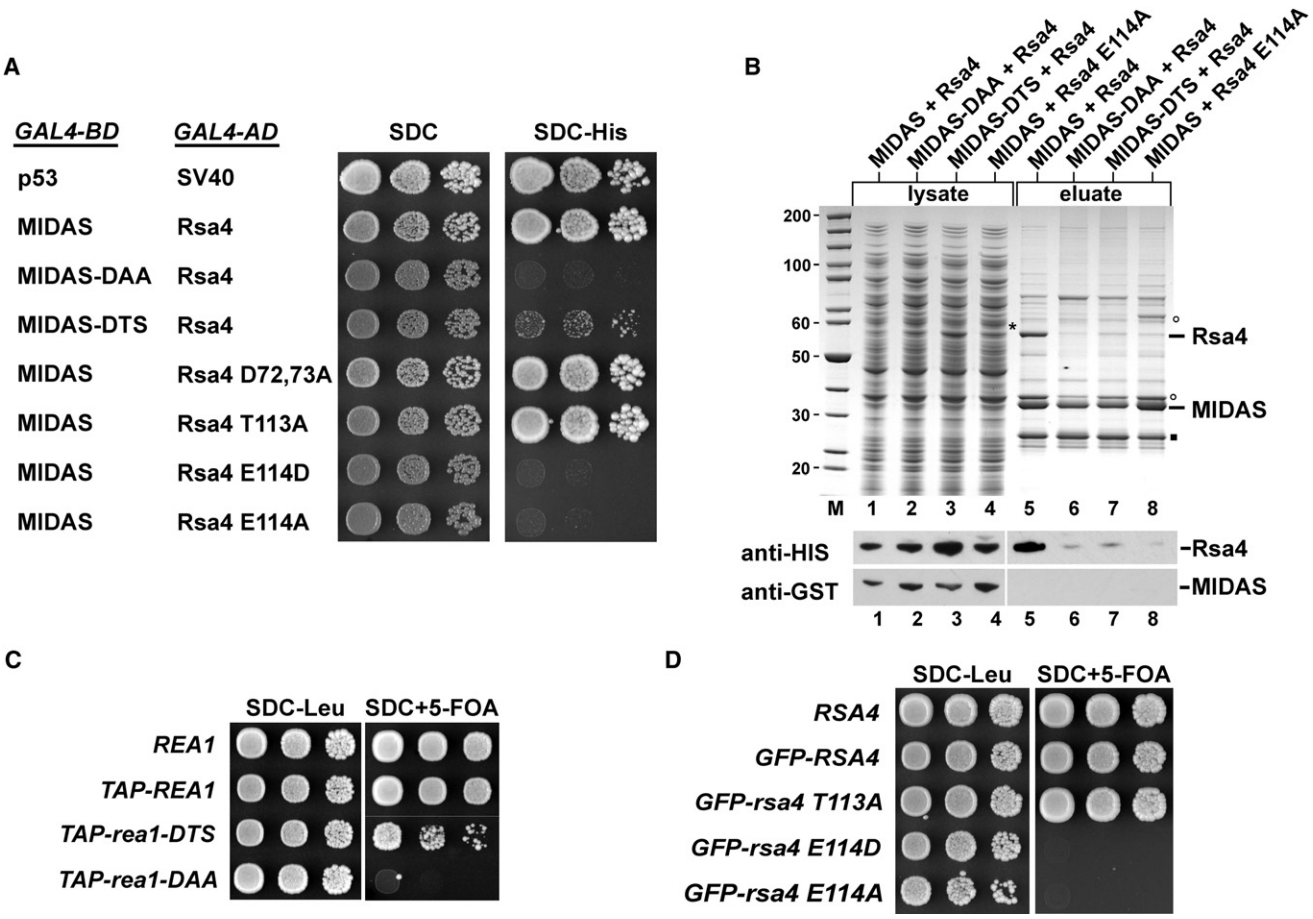

Figure 4. Physical Interaction Requires Critical Residues in the Rea1 MIDAS and Rsa4 N-Terminal Domain

(A) 2-hybrid interaction between the wild-type and mutant alleles of Rea1 MIDAS and Rsa4 N-domain. 2-hybrid plasmids expressing the indicated *GAL4-BD* and *GAL4-AD* constructs were transformed into the yeast reporter strain PJ69-4A. Transformants were spotted in 10-fold serial dilutions onto SDC-Trp-Leu (SDC) or SDC-Trp-Leu-His (SDC-His) plates and incubated at 30°C. The Rea1 MIDAS comprised residues 4620-4910, and the N-domain of Rsa4 residues 1–154.

(B) The Rea1 MIDAS and Rsa4 bind directly to each other. The GST-TEV-tagged MIDAS of Rea1 (either wild-type or the DAA and DTS mutants; residues 4608-4910) was co-expressed with HIS_6-tagged wild-type Rsa4 or the *rsa4 E114A* mutant in *E. coli* in the indicated combinations. Whole-cell lysates were prepared and the GST-MIDAS constructs were affinity-purified on GSH-beads and eluted by TEV-cleavage. Whole-cell lysates (1–4) and the corresponding eluates (5–8) were analyzed by SDS-PAGE and Coomassie staining (upper panel) or western blotting (lower panel) using anti-HIS antibodies to detect Rsa4 and anti-GST antibodies to detect the MIDAS (note that the GST antibody only reacts with the GST-MIDAS in the lysate but not in the eluate, where the GST tag was cleaved off by the TEV protease). The position of GST-MIDAS in the lysate is indicated by an asterisk, the TEV protease by a filled square and *E. coli* contaminants by open circles. Molecular weight marker (M).

(C and D) Growth analysis of the indicated *rea1* MIDAS (C) and *rsa4* mutants (D). Wild-type *REA1* and the *rea1* mutants mapping in the MIDAS domain and tagged with the TAP epitope were transformed into the *REA1* shuffle strain. Wild-type *RSA4* and the indicated *rsa4* mutants tagged with GFP were transformed into the *RSA4* shuffle strain. Transformants were spotted in 10-fold serial dilution steps onto SDC-Leu plates (to control the plating efficiency) and onto SDC+5-FOA plates (to check whether the mutations are lethal). Plates were incubated at 30°C for 3 days.

et al., 2005; Luo et al., 2007; Takagi, 2007). Consequently, we mutated the conserved DxSxS motif predicted to coordinate the MIDAS ion in Rea1 into DxTxS (MIDAS-DTS) or DxAxA (MIDAS-DAA) (Figure S3C). Whereas the single MIDAS-DTS mutant was viable although with a reduced cell growth, the MIDAS-DAA double mutant was lethal (Figure 4C). Importantly, the 2-hybrid and the biochemical interaction between these mutant forms of MIDAS and Rsa4 were significantly reduced (Figures 4A and 4B). In addition, the combination of a *rsa4* mutant allele (*rsa4-1*) with *rea1*-S4712T (MIDAS-DTS) caused a synthetic lethal phenotype (Figure S3D). Altogether these data demonstrate a strong physical and functional interaction between the Rea1 MIDAS and Rsa4.

Next, we searched for an essential acidic (aspartate or glutamate) residue in the Rsa4 N-domain that could provide the sixth coordination site of the MIDAS ion. We found that a conserved aspartic acid residue (E114) in the Rsa4 N-domain (Figure S4A) is essential for cell growth. Both, an *rsa4* E114D or E114A point mutation when introduced into the full-length protein could not rescue the lethal phenotype of the *rsa4Δ* strain (Figure 4D) and abolished the biochemical and the 2-hybrid interaction with the Rea1 MIDAS (Figures 4A and 4B). In contrast, mutating other

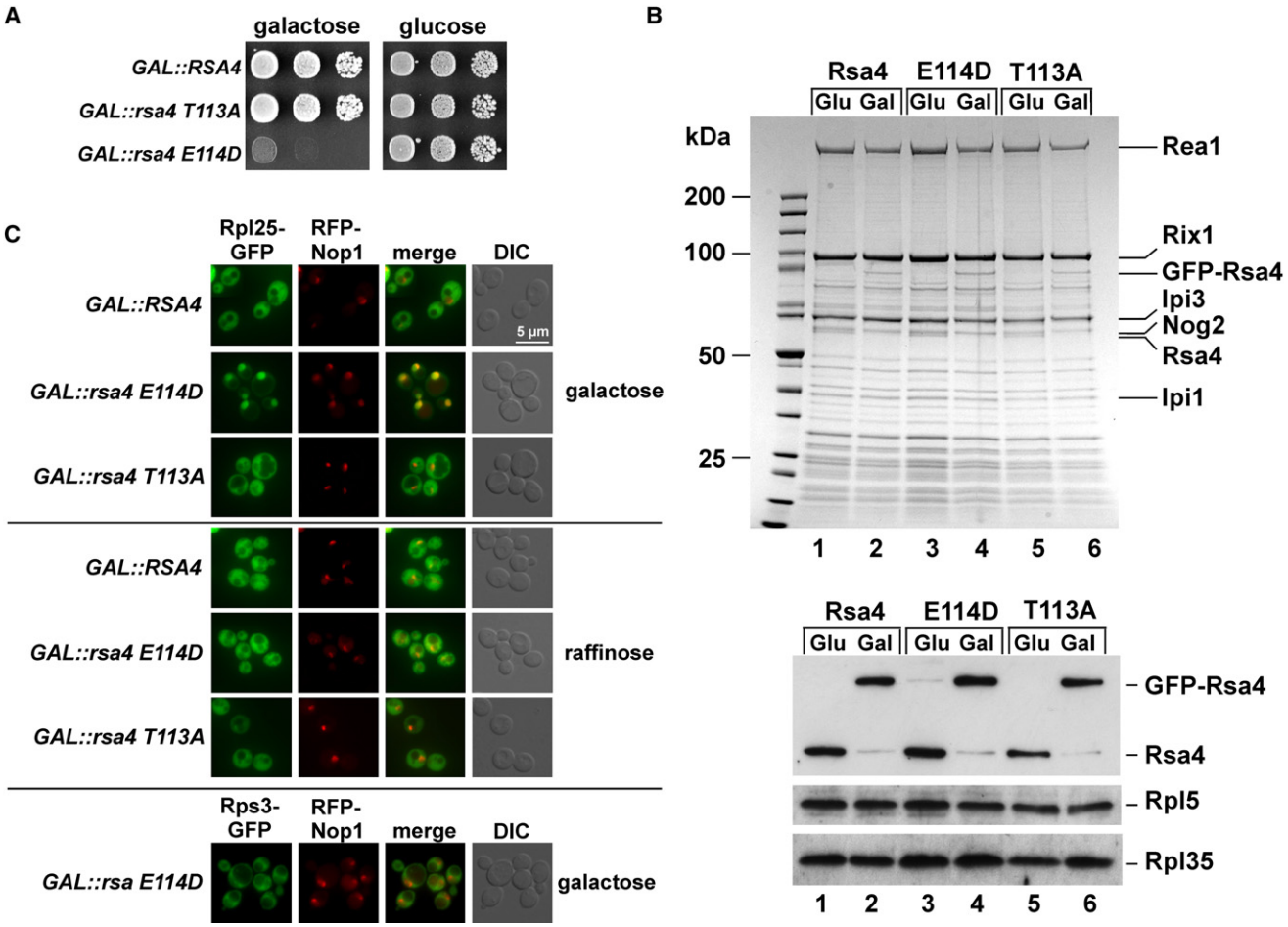

Figure 5. Mutation of the Conserved E114 in Rsa4 Generates a Dominant-Negative Phenotype and Inhibits 60S Subunit Formation

(A) The Rsa4 E114D mutation confers a dominant-negative phenotype. Wild-type *RSA4* and the indicated *rsa4 T113A* and *rsa4 E114D* mutant alleles were N-terminally GFP-tagged and expressed under the control of the inducible *GAL1* promoter in yeast. Transformants were spotted in 10-fold serial dilution steps onto SGC-Leu (galactose) and SDC-Leu (glucose) plates. Plates were incubated for 3 days at 30°C.

(B) Endogenous Rsa4 is displaced from the pre-60S subunit upon overexpression of the toxic *GAL::rsa4* E114D mutant. The yeast strain Y4294 strain was transformed with the constructs *GAL::RSA4*, *GAL::rsa4* E114D and *GAL::rsa4* T113A, respectively, which were tagged with GFP to distinguish them from endogenous Rsa4. Cells were grown for 6 h in glucose (Glu) or galactose (Gal) containing medium, before Rix1-TAP was affinity-purified and analyzed by SDS-PAGE and Coomassie staining (upper part) or western blotting (lower part) using an anti-Rsa4 antibody, which recognizes both the endogenous Rsa4 and overexpressed GFP-Rsa4. The Rpl5 and Rpl35 antibodies were used to probe for equal loading of the gel. Indicated on the right are prominent bands.

(C) Analysis of nuclear export of 60S and 40S subunits in the dominant-negative *GAL::rsa4 E114D* mutant (TAP-tagged). The indicated yeast strain (YDK11-5A) expressing either the 60S subunit reporter Rpl25-GFP or 40S subunit reporter Rps3-GFP was grown in galactose- or raffinose-containing medium at 30°C for 6 h, before the subcellular location of Rpl25-GFP and Rps3-GFP was analyzed by fluorescence microscopy. The strains also expressed mRFP-Nop1 as nucleolar marker. A merge between Rpl25-GFP or Rps3-GFP and mRFP-Nop1, as well as Nomarski (DIC) pictures are shown. The scale bar represents 5 µm.

conserved residues (T113A, D72A, D73A) did neither affect growth nor binding to Rea1 MIDAS (Figures 4A and 4D; data not shown). These findings suggest that E114 in the N-domain of Rsa4 provides the sixth coordination site for binding the MIDAS ion.

The importance of E114 in Rsa4 for the interaction with Rea1 and the overall 60S biogenesis is underscored by the observation that Rsa4 E114D overexpression under the *GAL* promoter exerts a dominant-lethal phenotype (Figures 5A and S4B). In contrast, cells overexpressing wild-type Rsa4 or the Rsa4 T113A mutation continued to grow normally in galactose-containing medium (Figures 5A and S4B). Biochemical analyses showed that overproduced Rsa4 E114D efficiently replaced the endogenous Rsa4 protein from its binding site on the pre-60S subunit without affecting significantly the overall biochemical composition (Figure 5B) and characteristic shape of the Rix1-particle (EM-analysis, data not shown). Moreover, in vivo analyses revealed that ribosome formation was inhibited upon overexpression of Rsa4 E114D. Specifically, late 7S to 5.8S rRNA processing was impaired (Figure S5) and pre-60S particles strongly accumulated in the nucleus (Figure 5C) causing a reduction of mature 60S subunits relative to 40S subunits and the appearance of "half-mer" polysomes in the cytoplasm (Figure S4C). These data suggest that Rsa4 binds to the preribosome prior

to interaction with the MIDAS domain and that the Rsa4 E114D mutant protein assembled into the Rix1-particle effectively blocks progression of the nascent pre-60S subunit and subsequent export to the cytoplasm.

Interaction between Rea1 MIDAS and Rsa4 Is Required for Their ATP-Dependent Release from the Pre-60S Particle

We next asked whether the MIDAS-Rsa4 interaction is coupled with Rea1's ATPase function. Previously, we observed that when Rix1-TAP was affinity-purified and treated with ATP, Rea1 and to a lesser extent also ribosomal 60S proteins (Rpl) were dissociated from the Rix1-Ipi1-Ipi3 complex (Nissan et al., 2004). To test whether this ATP-dependent release of Rea1 depends on the MIDAS-Rsa4 contact we affinity-purified Rix1-TAP from cells harboring either wild-type Rsa4 or mutated Rsa4 E114D in the presence of ATP. Strikingly, pre-60S particles carrying mutant Rsa4 E114D were inert toward ATP-treatment since neither pre-60S factors (e.g., Rsa4 E114D, Rea1, Nog1 and Nog2) nor 60S subunit proteins (Rpl) were released from the immobilized Rix1-Ipi1-Ipi3 complex (Figure 6A, lane 4). In contrast, these pre-60S factors and a significant amount of Rpl proteins were dissociated from the Rix1-subcomplex upon ATP incubation in the case of wild-type Rsa4 (Figure 6A, lane 3). However, incubation with the non-hydrolyzable ATP analog AMP-PNP did not promote release of the pre-60S factors and ribosomal proteins from the wild-type Rix1-particle suggesting that ATP hydrolysis is required for the dissociation step (Figure 6A, lane 5).

The in vitro assay employed so far (see Nissan et al., 2004) revealed ATP-dependent dissociation of factors and Rpl proteins from the purified Rix1-subcomplex, but did not monitor whether the released non-ribosomal factors were still associated with the ribosomal Rpl proteins (i.e., 60S subunits). To address this point, we extended our in vitro assay. The pre-60S particle was tandem affinity-purified via Rix1-TAP from wild-type cells and the final EGTA eluate was incubated with or without ATP. Subsequently, the entire reaction mixtures were analyzed by sucrose gradient centrifugation. In the mock-treated sample (-ATP), Rea1, Rsa4 and the Rix1-subcomplex significantly co-sedimented with the 60S subunit on the sucrose gradient (Figure 6B, fraction 10). However, a pool of the Rix1-subcomplex devoid of Rpl proteins was also recovered in the upper part of the sucrose gradient, which corresponds to the free Rix1-Ipi1-Ipi3 heterotrimer known to exist in yeast (Krogan et al., 2004). In the ATP-treated sample Rea1 and Rsa4 were efficiently released from the pre-60S particle and recovered in the upper part of the sucrose gradient but in different fractions. The Rix1-subcomplex was also released from the 60S subunit upon ATP-treatment, but not completely and a residual pool remained bound (Figure 6B and Figure S6; see also Discussion). In contrast, other pre-60S factors including Nog1, Nog2, Nsa2, Rlp24, Nop7 and Tif6 were not released by ATP treatment and co-sedimented with the 60S subunit (Figure 6B and data not shown). Consistent with this data, Nsa2 is still present on the Arx1-particle that evolved from the Rix1-particle during 60S subunit biogenesis (see also Figure 3B). Altogether, the data suggest that an interaction between the Rea1 MIDAS and Rsa4 is necessary for ATP-dependent dissociation of a group of preribosomal factors from the 60S subunit (i.e., Rea1, Rsa4, Rix1-subcomplex), whereas other factors present on the Rix1-particle (see above) apparently were not released. Thus, these latter factors could require other mechanisms for their removal from the evolving pre-60S particle (see also Discussion).

Finally, we investigated which morphological changes were induced by ATP-treatment of the Rix1-particle. Rix1-particles were applied to EM-grids and incubated with ATP before staining for subsequent EM analysis and image processing. Comparison and quantification of class averages of ATP-treated and untreated samples revealed that ATP caused a significant increase of tail-less (from 29% to 64%) and a corresponding decrease (from 71% to 36%) in tail-containing pre-60S particles (Figure 6C and Figure S1). Concomitantly, ATP-treatment induced a ~3-fold increase in smaller fragments that were apparently released from the Rix1-particles (Figure S1C). The analysis of the ATP-treated sample revealed that 20% of these smaller fragments clustered into classes that resembled Rea1 molecules, which were largely absent in the untreated sample (Figure 6C, Figure S1). Other fragments generated by ATP-treatment formed classes that were similar in the treated and untreated sample and could represent the dissociated Rix1-subcomplex (Figure S1; see Discussion). Incubation of Rix1-particles with AMP-PNP did neither induce major structural changes of the particles nor cause a release of Rea1 (M.D., unpublished data). In conclusion, the ATP-induced decrease of tail-containing particles together with the increase of smaller fragments, one of them being clearly Rea1, agrees well with the biochemical data and is consistent with a model of an ATP-dependent release of preribosomal factors from the Rix1-particle.

DISCUSSION

This study has uncovered a mechanochemical constellation of biogenesis factors on the surface of a distinct pre-60S particle that allows ATP-dependent remodeling of the nascent 60S subunit prior to nuclear export. Our EM data demonstrate that the AAA domain of Rea1 is fixed at the Rix1-particle, whereas the Rea1 tail is flexible with respect to the 60S moiety and can move toward a region on the pre-60S subunit where Rsa4 is located (Figure 7). Moreover, the EM data indicate that Rea1 consists of two major structural entities, a ring domain that is connected to the body possibly involving the Rix1-subcomplex and a ~15 nm long tail protruding from the AAA domain. Thus, Rea1's head domain, which harbours the six AAA protomers, could form a hexameric ring structure in analogy to the AAA domain of dynein (Roberts et al., 2009).

The Rea1 tail is intrinsically flexible and probably also hinged in respect to the preribosomal particle as suggested by the different angular mobility observed in the Rea1 molecule. This mobility of the tail enables the tail to loop back onto the preribosome as seen in some selected particles (Figure 1D and Movies S1 and S2). Currently, it is unclear whether the movement of Rea1 toward Rsa4 and/or their subsequent interaction is regulated, e.g., by a GTPase, or whether similar to the priming of the dynein heavy chain (Roberts et al., 2009) is driven by binding of ATP to the motor domain that moves the tail toward Rsa4.

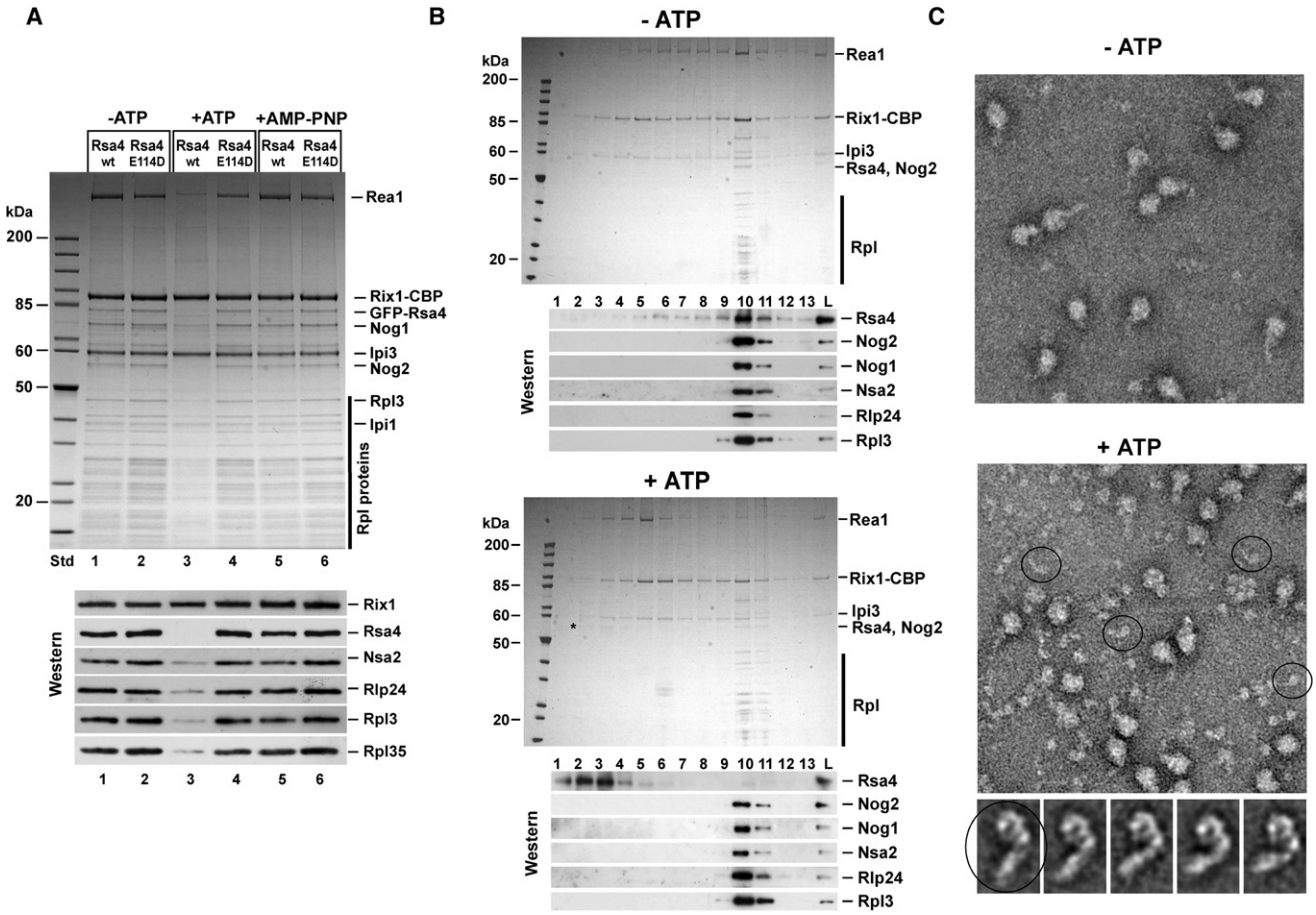

Figure 6. ATP-Dependent Release of Rsa4, Rea1, and the Rix1-Subcomplex from the Pre-60S Particle

(A) The MIDAS-Rsa4 interaction is required for ATP-dependent release of Rea1, Rsa4, and Rpl proteins from the Rix1-subcomplex. Rix1-TAP was affinity-purified from cells expressing GFP-Rsa4 (wild-type, wt) or mutant GFP-Rsa4 E114D. During TEV-cleavage and the successive purification steps 2 mM ATP, 2 mM AMP-PNP, or mock buffer (-ATP) was added. After EGTA elution from the final calmodulin beads, the Rix1-TAP preparations were analyzed by SDS-PAGE and Coomassie staining (upper part) or western blotting (lower part) using anti-CBP (to detect the Rix1-CBP bait), anti-Rsa4 (to detect GFP-Rsa4), anti-Nsa2, anti-Rlp24, anti-Rpl3, and Rpl35 antibodies.

(B) Release of non-ribosomal factors from the pre-60S particle by ATP-treatment monitored by sucrose gradient centrifugation. The Rix1-particle was tandem affinity-purified and the final EGTA eluate was incubated with 2 mM ATP for 2 hr at 16°C before loading the whole mixture on a sucrose gradient (5%–30%). After centrifugation for 15 hr at 27,000 rpm, the gradient was fractionated, and the gradient fractions 1-13 and the load fraction (L) were analyzed by SDS-PAGE and Coomassie staining (upper part) or western blotting using the indicated antibodies (lower part). The band labeled by a star indicates the ATP-released Rsa4.

(C) ATP-dependent release of Rea1 from the Rix1-particle followed by electron microscopy. Rix1-particles affinity-purified via Rix1-TAP were immobilized on EM-grids and incubated with 2 mM ATP before staining for subsequent electron microscopy. Comparison of negatively stained mock-treated (-ATP) and ATP-treated (+ATP) sample revealed an increase of tail-less and decrease of tail-containing particles as well as an increase of smaller fragments (for quantification see Figure S1C). Some of these fragments resembled Rea1 molecules (circle), which were further analyzed by alignment and classification (lower panel gallery; see Figure S1 for overview). Some of these class averages corresponding to released Rea1 showed the same projection of the globular domain but grouped into classes with different tail positions indicating intrinsic flexibility of Rea1.

Fixation of the long Rea1 molecule at two distinct sites on the preribosomal surface is finally achieved by binding of MIDAS in Rea1 to Rsa4. In this constellation, a tension force could be generated by ATP hydrolysis in the AAA-ATPase motor domain, which is vectorially transmitted into the pre-60S particle for structural rearrangement (Figure 7).

An alternative to a spring-like tension model (Figure 7) is a long-range cooperative communication between the AAA head and the MIDAS domain. In such a scenario the long Rea1 tail could couple the two functional activities by transmitting structural information between the motor head and the substrate binding site at the MIDAS domain. Thus, propagation of information between AAA head and MIDAS via the tail could coordinate Rsa4 binding with the ATPase function. This mechanism would be similar to the binding of microtubules to the dynein heavy chain. There, a conformational change in dynein's microtubule-binding domain is transmitted toward the ATPase domain via the relative sliding of two α helices within the stalk (Carter et al., 2008).

Integrins utilize a MIDAS to bind to their extracellular ligands. Our mutational analysis suggests a similar binding mechanism

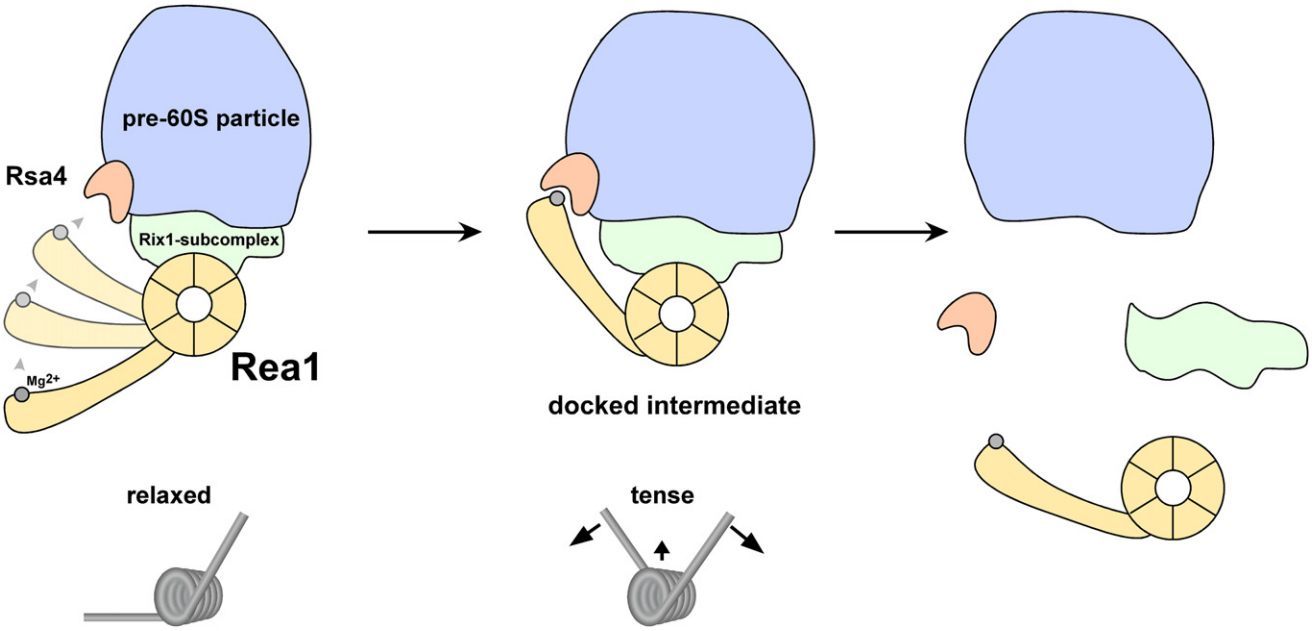

Figure 7. Model of a Mechanochemical Device on the Pre-60S Subunit to Generate Tensile Force for Removal of Pre-60S Factors

Schematic drawing of the pre-60S particle with attached Rea1 (composed of a hexameric AAA ATPase ring and a protruding tail) and Rsa4 (with a MIDAS binding site). Rsa4, Rea1 and the Rix1-subcomplex are released in an ATP-dependent manner. The tip of the flexible Rea1 tail harbours the MIDAS domain, which coordinates the MIDAS ion (Mg^{2+}). The AAA ring of Rea1 is attached via an adaptor structure (Rix1-subcomplex) to the 60S moiety, but the MIDAS tail can move up and contact the pre-60S particle at a distant site where Rsa4 is located. In a hypothetical pre-60S intermediate (middle panel), the MIDAS is docked to Rsa4 and hence tensile force generated by ATP hydrolysis in the Rea1 AAA domain can be used to pull off Rsa4, the Rix1-subcomplex and Rea1 from the pre-60S particle (right panel). The two different states of the Rea1 molecule (tail not bound and bound to Rsa4, respectively) are compared to a tensile spring in its relaxed or loaded (tense) state.

between Rea1 and Rsa4. The MIDAS domain of integrins harbors a ratchet-like α-helix that undergoes a conformational change (between open and close state) upon ligand binding. This effect is then transmitted toward a neighboring domain and finally through the entire integrin molecule into the cell (''outside-in signaling'') (Arnaout et al., 2005; Luo et al., 2007). The critical α-helix undergoing rearrangement upon ligand binding is also conserved in the Rea1 MIDAS domain. Moreover, it was shown that integrin MIDAS-ligand interactions have to resist mechanical tension and are further stabilized under tension (Craig et al., 2004; Astrof et al., 2006). In analogy, the initial contact between MIDAS and Rsa4 on the pre-60S particle could be strengthened by a pulling force generated by the Rea1 motor domain, allowing the unrestricted transmission of power onto the pre-60S particle for remodeling, which eventually leads to the dissociation of Rea1, Rsa4 and the Rix1-complex from the preribosome. After this release tension becomes reduced, which in consequence could weaken the interaction between MIDAS and Rsa4. In agreement with this speculation, Rea1 and Rsa4 released from the 60S subunit after ATP-treatment were found in different fractions of the sucrose gradient and class averages of the released Rea1 did not show an enlarged tip of the tail as would be expected if Rsa4 would remain bound.

In vitro the Rix1-subcomplex was only partially released from the pre-60S particle upon ATP treatment, whereas Rsa4 and Rea1 were dissociated very effectively. We attribute this difference to the fact that only two third of the Rix1-particles carry the Rea1 AAA ATPase (i.e., tail-containing particles). Assuming that only the concerted action between the Rea1 MIDAS and Rsa4 will lead to an ATP-dependent removal of the Rix1-subcomplex from the particle, the Rix1-subcomplex bound to tailless pre-60S subunits may not be detachable in vitro. Whether the Rix1-particles lacking Rea1 are bona fide pre-60S intermediates or some Rea1 molecules fall off during the prolonged purification procedure is not clear.

Our data are consistent with a model in which the Rix1-subcomplex is attached to the interface region of the 60S moiety, which later on during 60S biogenesis (i.e., at the level of the Arx1-particle) recruits the export factors Nmd3, Crm1 and Mex67-Mtr2 (Yao et al., 2007). Therefore, the ATP-dependent clearance of preribosomal factors from this surface could trigger the final nuclear biogenesis steps, which include structural rearrangement of pre-rRNA including 7S to 5.8S rRNA processing and unmasking of binding sites for export receptors. Thus, the generation of a tensile force by the Rea1 AAA ATPase could provoke structural maturation of a late nuclear pre-60S particle to generate the export-competent large subunit. Since ATP treatment did not release all preribosomal factors from the Rix1-particle (e.g., Nog1, Nog2, Nsa2, Rlp24, Nop7, Tif6), additional steps are needed for final maturation of the 60S subunit. One candidate factor is another AAA ATPase, Drg1, which was reported to trigger the release of a number of shuttling preribosomal factors (e.g., Nog1, Rlp24, Tif6, Arx1) from the pre-60S particles in the cytoplasm shortly after nuclear export (Pertschy et al.,

2007). Moreover, other reported release factors (e.g., Rpl10, Sqt1, Rei1, Jjj1) including GTPases (Lsg1 and Elf1) were implicated in the final dissociation and recycling of a number of pre-60S factors such as Nmd3, Arx1, Alb1 and Tif6 in the cytoplasm (for review see Henras et al., 2008; Zemp and Kutay, 2007).

In conclusion, rather than involving a cytoskeletal filament, the dynein-related Rea1 AAA ATPase and its interacting partners form a proper mechanochemical arrangement on the Rix1 pre-60S particle to exert a power stroke that can be used to release preribosomal factors and generate the export-competent 60S subunit.

EXPERIMENTAL PROCEDURES

Strains, Media, and Plasmids

Plasmids used in this study were generated using standard procedures and are listed in Table S2. Yeast *Saccharomyces cerevisiae* strains used in this study are listed in Table S3. The *Rea1/Rsa4* double shuffle strain was generated according to (Sträßer et al., 2000). Yeast genetic methods such as gene deletion or epitope tagging (TAP, HA, GFP) of genes at the genomic locus, transformation, mating and tetrad analysis were performed according to published procedures (Baßler et al., 2001; Longtine et al., 1998; Puig et al., 1998).

Protein Purification, Antibody Labeling, and Electron Microscopy

Rea1 was fused N-terminally with a TAP-tag expressed from a plasmid under control of the *GAL1* promoter in a wild-type yeast strain. Cells were grown in galactose-containing (YPG) medium to induce Rea1 overexpression. TAP-Rea1 was purified according to (Nissan et al., 2002), except that the buffers used for incubation on the calmodulin beads and the subsequent wash step contained 2 mM ATP for release of Rea1 from the preribosomal particles.

For immuno-EM, purification of Rix1-particles and antibody binding were performed as described (Nissan et al., 2002). For Ipi3-HA labeling the preribosomes were purified via Ipi3-HA-TAP, which yields the same type of particle (Nissan et al., 2004).

All negatively stained samples of Rea1 and the Rix1-particle were prepared with the sandwich technique as described (Diepholz et al., 2008). Particles were imaged under low dose using a Philips CM200 FEG electron microscope with a 2k x 2k CCD camera (TVIPS-GmbH) or using a Tecnai F30 electron microscope with a 4k x 4k Eagle camera (Table S1, for imaging conditions).

Image Processing

Particle images were selected from micrographs using 'Boxer' (Ludtke et al., 1999). Further image processing was done with IMAGIC 5 (van Heel et al., 1996). Particles were band-pass filtered and normalized in their gray value distribution. Unlabelled Rix1-particles were mass-centered, and classified following the alignment by classification strategy (Dube et al., 1993), whereas antibody-labeled Rix1-particles were aligned to a set of references. The set of references included one class average of tail-containing particles of group1 and one of group 2 (Figure 1C, S1 for grouping) and their mirror images. For labeled and unlabeled Rix1-particles alignment was followed by multivariate statistical analysis (MSA). For labeled Rix1-particles only those particles were retained in the data set, which grouped into classes resembling class averages of group 1 or group 2. Alignment and classification were repeated until classes remained stable (usually 1–2 iterations).

Finally for labeled particles, the aligned dataset was classified using a mask that focused the classification onto the periphery of the particle. This approach identified areas where additional density at the perimeter appeared frequently, but could not distinguish between small changes in the orientation of the body. However, due to preselection of particle images that belonged to group 1 or group 2 the orientational variations were relatively small.

To determine the distribution of the tail angles in the stained Rix1-particles (Figure 1D) these images were aligned to a representative set of class averages of tail containing particles, where the tails were computationally removed by a tight mask. Particle images that aligned to the same reference were sub-classified with a new mask only including the tail region. For accessing the intrinsic flexibility of Rea1 molecules (Figures 1B and 6C), only particle views that exhibited a regular ring-shaped domain were used. Class averages of these particles, including only the ring domain and the short tail-segment, were aligned relative to each other and used as references. Aligned particle images were classified using MSA focused on the ring domain (tight circular mask). Particles that grouped into the same class were sub-classified taking the whole particle into account (larger circular mask).

Miscellaneous

Reconstitution of the MIDAS-Rsa4 Interaction in *E. coli* and their subsequent affinity-purification were performed essentially as described (Gadal et al., 2001) with modifications given in the Supplemental Data. The preparation of rRNA and Northern blot analysis, and ATP treatment of the Rix1-particle are described in the Supplemental Data. Additional methods used in this study and described earlier include TAP-purification of pre-60S particles (Baßler et al., 2001; Nissan et al., 2002), sucrose gradient analysis to obtain ribosomal and polysomal profiles (Baßler et al., 2001), ribosomal export assays using the large subunit reporter Rpl25-GFP (Gadal et al., 2002) and the small subunit reporter Rps3-GFP (Milkereit et al., 2002) monitored by fluorescence microscopy according to (Baßler et al., 2006) and yeast 2-hybrid analysis (Kressler et al., 2008).

SUPPLEMENTAL DATA

Supplemental Data include Supplemental Experimental Procedures, six figures, two movies, and three tables and can be found with this article online at http://www.cell.com/supplemental/S0092-8674(09)00792-2.

ACKNOWLEDGMENTS

The excellent technical help of Martina Kallas and Claire Batisse is gratefully acknowledged. We thank Drs. M. Remacha, H. Tschochner, M. Fromont-Racine, A. W. Johnson, M. Seedorf, B. Stillman, and J. Warner for antibodies. B.B. was supported by the EU-grant '3D repertoire (LSHG-CT-2005-512028) and by the Welcome Trust (WT 087658). M.D. was supported by an E-STAR project (FP6 Marie Curie Action for Early-Stage-Training, MEST-CT-2004-504640). E.H. and J.B. are recipients of grants from the Deutsche Forschungsgemeinschaft (Hu363/9-2) and Fonds der Chemischen Industrie.

Received: October 16, 2008
Revised: May 11, 2009
Accepted: June 17, 2009
Published: September 3, 2009

REFERENCES

Arnaout, M.A., Mahalingam, B., and Xiong, J.P. (2005). Integrin structure, allostery, and bidirectional signaling. Annu. Rev. Cell Dev. Biol. *21*, 381–410.

Astrof, N.S., Salas, A., Shimaoka, M., Chen, J., and Springer, T.A. (2006). Importance of force linkage in mechanochemistry of adhesion receptors. Biochemistry *45*, 15020–15028.

Baßler, J., Grandi, P., Gadal, O., Leßmann, T., Tollervey, D., Lechner, J., and Hurt, E.C. (2001). Identification of a 60S pre-ribosomal particle that is closely linked to nuclear export. Mol. Cell *8*, 517–529.

Baßler, J., Kallas, M., and Hurt, E. (2006). The NUG1 GTPase reveals and N-terminal RNA-binding domain that is essential for association with 60 S pre-ribosomal particles. J. Biol. Chem. *281*, 24737–24744.

Carter, A.P., Garbarino, J.E., Wilson-Kubalek, E.M., Shipley, W.E., Cho, C., Milligan, R.A., Vale, R.D., and Gibbons, I.R. (2008). Structure and functional role of dynein's microtubule-binding domain. Science *322*, 1691–1695.

Chantha, S.C., and Matton, D.P. (2006). Underexpression of the plant NOTCH-LESS gene, encoding a WD-repeat protein, causes pleitropic phenotype during plant development. Planta *225*, 1107–1120.

Craig, D., Gao, M., Schulten, K., and Vogel, V. (2004). Structural insights into how the MIDAS ion stabilizes integrin binding to an RGD peptide under force. Structure *12*, 2049–2058.

Diepholz, M., Venzke, D., Prinz, S., Batisse, C., Flörchinger, B., Rössle, M., Svergun, D.I., Böttcher, B., and Féthière, J. (2008). A different conformation for the EGC stator sub-complex in solution and in the assembled yeast V-ATPase. Structure *16*, 1789–1798.

Dube, P., Tavares, P., Lurz, R., and van Heel, M. (1993). The portal protein of bacteriophage SPP1: a DNA pump with 13-fold symmetry. EMBO J. *12*, 1303–1309.

Erzberger, J.P., and Berger, J.M. (2006). Evolutionary relationships and structural mechanisms of AAA+ proteins. Annu. Rev. Biophys. Biomol. Struct. *35*, 93–114.

Fromont-Racine, M., Senger, B., Saveanu, C., and Fasiolo, F. (2003). Ribosome assembly in eukaryotes. Gene *313*, 17–42.

Gadal, O., Strauß, D., Kessl, J., Trumpower, B., Tollervey, D., and Hurt, E. (2001). Nuclear export of 60S ribosomal subunits depends on Xpo1p and requires a NES-containing factor Nmd3p that associates with the large subunit protein Rpl10p. Mol. Cell. Biol. *21*, 3405–3415.

Gadal, O., Strauss, D., Petfalski, E., Gleizes, P.E., Gas, N., Tollervey, D., and Hurt, E. (2002). Rlp7p is associated with 60S preribosomes, restricted to the granular component of the nucleolus, and required for pre-rRNA processing. J. Cell Biol. *157*, 941–951.

Galani, K., Nissan, T.A., Petfalski, E., Tollervey, D., and Hurt, E. (2004). Rea1, a Dynein-related Nuclear AAA-ATPase, Is Involved in Late rRNA Processing and Nuclear Export of 60 S Subunits. J. Biol. Chem. *279*, 55411–55418.

Garbarino, J.E., and Gibbons, I.R. (2002). Expression and genomic analysis of midasin, a novel and highly conserved AAA protein distantly related to dynein. BMC Genomics *3*, 18–28.

Granneman, S., and Baserga, S.J. (2004). Ribosome biogenesis: of knobs and RNA processing. Exp. Cell Res. *296*, 43–50.

Henras, A.K., Soudet, J., Gerus, M., Lebaron, S., Caizergues-Ferrer, M., Mougin, A., and Henry, Y. (2008). The post-transcriptional steps of eukaryotic ribosome biogenesis. Cell. Mol. Life Sci. *65*, 2334–2359.

Kressler, D., Roser, D., Pertschy, B., and Hurt, E. (2008). The AAA ATPase Rix7 powers progression of ribosome biogenesis by stripping Nsa1 from pre-60S particles. J. Cell Biol. *181*, 935–944.

Krogan, N.J., Peng, W.T., Cagney, G., Robinson, M.D., Haw, R., Zhong, G., Guo, X., Zhang, X., Canadien, V., Richards, D.P., et al. (2004). High-definition macromolecular composition of yeast RNA-processing complexes. Mol. Cell *13*, 225–239.

Longtine, M.S., McKenzie, A., Demarini, D.J., Shah, N.G., Wach, A., Brachat, A., Philippsen, P., and Pringle, J.R. (1998). Additional modules for versatile and economical PCR-based gene deletion and modification in Saccharomyces cerevisiae. Yeast *10*, 953–961.

Ludtke, S.J., Baldwin, P.R., and Chiu, W. (1999). EMAN: semiautomated software for high-resolution single-particle reconstructions. J. Struct. Biol. *128*, 82–97.

Luo, B.H., Carman, C.V., and Springer, T.A. (2007). Structural basis of integrin regulation and signaling. Annu. Rev. Immunol. *25*, 619–647.

Milkereit, P., Strauß, D., Baßler, J., Gadal, O., Kühn, H., Schütz, S., Gas, N., Lechner, J., Hurt, E., and Tschochner, H. (2002). A Noc-complex specifically involved in the formation and nuclear export of ribosomal 40S subunits. J. Biol. Chem. *278*, 4072–4081.

Nissan, T.A., Baßler, J., Petfalski, E., Tollervey, D., and Hurt, E.C. (2002). 60S pre-ribosome formation viewed from assembly in the nucleolus until export to the cytoplasm. EMBO J. *21*, 5539–5547.

Nissan, T.A., Galani, K., Maco, B., Tollervey, D., Aebi, U., and Hurt, E. (2004). A pre-ribosome with a tadpole-like structure functions in ATP-dependent maturation of 60S subunits. Mol. Cell *15*, 295–301.

Pertschy, B., Saveanu, C., Zisser, G., Lebreton, A., Tengg, M., Jacquier, A., Liebminger, E., Nobis, B., Kappel, L., van der Klei, I., et al. (2007). Cytoplasmic recycling of 60S preribosomal factors depends on the AAA protein Drg1. Mol. Cell. Biol. *27*, 6581–6592.

Puig, O., Rutz, B., Luukkonen, B.G., Kandels-Lewis, S., Bragado-Nilsson, E., and Seraphin, B. (1998). New constructs and strategies for efficient PCR-based gene manipulations in yeast. Yeast *14*, 1139–1146.

Roberts, A.J., Numata, N., Walker, M.L., Kato, Y.S., Malkova, B., Kon, T., Ohkura, R., Arisaka, F., Knight, P.J., Sutoh, K., et al. (2009). AAA+ Ring and linker swing mechanism in the dynein motor. Cell *136*, 485–495.

Spahn, C.M., Beckmann, R., Eswar, N., Penczek, P.A., Sali, A., Blobel, G., and Frank, J. (2001). Structure of the 80S ribosome from Saccharomyces cerevisiae–tRNA-ribosome and subunit-subunit interactions. Cell *107*, 373–386.

Sträßer, K., Baßler, J., and Hurt, E.C. (2000). Binding of the Mex67p/Mtr2p heterodimer to FXFG, GLFG, and FG repeat nucleoporins is essential for nuclear mRNA export. J. Cell Biol. *150*, 695–706.

Takagi, J. (2007). Structural basis for ligand recognition by integrins. Curr. Opin. Cell Biol. *19*, 557–564.

Tschochner, H., and Hurt, E. (2003). Pre-ribosomes on the road from the nucleolus to the cytoplasm. Trends Cell Biol. *13*, 255–263.

Vale, R.D. (2000). AAA proteins: lords of the ring. J. Cell Biol. *150*, 13–19.

van Heel, M., Harauz, G., Orlova, E.V., Schmidt, R., and Schatz, M. (1996). A new generation of the IMAGIC image processing system. J. Struct. Biol. *116*, 17–24.

Yao, W., Roser, D., Köhler, A., Bradatsch, B., Baßler, J., and Hurt, E. (2007). Nuclear export of ribosomal 60S subunits by the general mRNA export receptor Mex67-Mtr2. Mol. Cell *26*, 51–62.

Zemp, I., and Kutay, U. (2007). Nuclear export and cytoplasmic maturation of ribosomal subunits. FEBS Lett. *581*, 2783–2793.